25

INTERNATIONAL JOURNAL FOR NUMERICAL METHODS IN ENGINEERING, VOL. 17, 1823–1833

QUASISTATIC INDENTATION OF A RUBBER-COVERED ROLL BY A RIGID ROLL

R. C. BATRA

Department of Engineering Mechanics, University of Missouri-Rolla, Rolla, U.S.A.

SUMMARY

The nonlinear elastic problem involving the indentation of a slightly compressible rubber-like layer bonded to a rigid cylinder and indented by another rigid cylinder is analysed by the finite element method. Both the geometric and material nonlinearities are accounted for. The finite element formulation of the problem is based upon a variational principle recently proposed by Cescotto and Fonder, and is valid for both slightly compressible and incompressible materials. The results computed and presented graphically include the shape of the indented surface, the pressure distribution over the contact surface, and the stress distribution at the bond surface. For the same contact width, the results for the compressible material are found to differ significantly from those for the case when the rubber-like layer is assumed to be incompressible.

INTRODUCTION

Traction in vehicles, the nip action in cylindrical rolls in the paper-making process and in the textile industry, and friction drives are some examples of the kind of problem studied herein. Each of these problems involves indentation, by a steel or granite cylinder, of a rubber-like layer bonded to a cylindrical core made also of steel or granite. Such a problem has been solved by Batra *et al.*[1] by using the finite element method and the assumption that the rubber-like layer is made of a linear viscoelastic material. Hahn and Levinson[2] used the Airy stress function to solve the linear elastic problem. In order to explore the effects of material and geometric nonlinearities, Batra[3] recently studied the problem in which the rubber-like layer is assumed to be made of a homogeneous Mooney–Rivlin material. Even though results presented here and in References 1 and 3 are for one specific geometry of the rolls, the formulation of the problem and the method of solution is applicable to all possible geometries, i.e. the thickness of the rubber-like layer is small/large as compared to the roll diameter, and the mating cylinders are of comparable or widely different diameters. Experimental work involving varying thickness of the rubber-like layer and different combinations of the diameters of mating cylinders has been done by Spengos.[4] However, the only material property listed for the rubber is the durometer hardness. For the linear elastic problem involving incompressible material, the durometer hardness is enough to find Young's modulus and hence solve the problem. Since the reported values of maximum strain and also those encountered in practice far exceed the usually accepted range of validity of the linear theory, the nonlinear analysis is necessary. For literature on related problems, we refer the reader to works cited in References 1–4.

Whereas in the earlier study of the nonlinear problem the rubber-like layer is assumed to be incompressible, in the present work the layer is taken to be made of a slightly compressible material. That the compressibility of the material has a noticeable effect on the pressure

0029–5981/81/121823–11$01.10

Received 7 August 1980
Revised 16 January 1981

distribution at the contact surface and the stress distribution at the bond surface is evidenced by the work of Hahn and Levinson[2] and Meijers,[5] and is also confirmed by results obtained herein. Both Hahn and Levinson and Meijers assume that the deformations are small and the linear theory applies. Other factors motivating the present study are that real rubbers are slightly compressible and finite element analysis of nonlinear problems involving nearly incompressible materials is quite different from that involving either compressible or perfectly incompressible materials. Also, it is hoped that the improved understanding of the stress distribution within the covering layer and at the bond surface and the deformed shape of the layer will lead to design standards which, if followed, would result in longer covering layer life.

In formulating a problem for nearly incompressible material, Skala[6] models rubber-like solids by the constitutive equation

$$W = C_1(I_1 - I_3 - 2) + C_3(\sqrt{(I_3)} - 1)^2$$

in which W is the strain energy density, C_1 and C_3 are material constants and I_1, I_3 are first and third invariants of the right Cauchy–Green strain tensor. Using the minimum energy principle and 8-node isoparametric element, the problem of inflation of a cylindrical pressure vessel is solved. Although reduced numerical integration technique as suggested by Naylor[7] was used, some oscillations in the calculated stresses as the material became more incompressible were noticed. In Reference 8, Hughes *et al.* use as constitutive law

$$W = \tfrac{1}{2}\lambda(\ln\sqrt{I_3})^2 + rE_{ij}E_{ij}$$

where λ and r are material constants, E_{ij} is the strain tensor defined below and the summation convention is used. For nearly incompressible materials, λ is taken to be large.

In this paper, the variational principle proposed recently by Cescotto and Fonder[9] is used in the finite element formulation of the problem. In this approach, the displacements at each nodal point and the dilation within each element are assumed to be unknown. Necessary equations to solve for these unknowns are obtained by seeking the extremum of a functional involving the strain energy density and the work done by applied loads. The 4-node isoparametric quadrilateral elements with 2×2 Gaussian integration rule are used. The dilation is assumed to be constant within each element. Since this formulation is valid for both compressible and incompressible materials, the accuracy of the developed code is established by solving two finite strain problems, namely, inflation of a thick-wall pressure vessel and the contact problem for the roll cover, assuming in each case that the rubber-like material is incompressible. The computed results agreed very well with those obtained from the analytic solution[10] for the pressure vessel problem and those obtained earlier[3] for the roll cover problem. A pressure vessel problem for compressible materials and involving infinitesimal strains was also solved and results were found to compare well with the analytical solution.

For the roll cover problem, the computed results show that, for the same value of contact width in the reference configuration, the indentation is 10 per cent more for the case when Poisson's ratio in the undeformed state for the rubber-like layer is 0·45 than when it is made of an incompressible material. Also considerably less load is needed to cause the same contact width in the compressible case.

FORMULATION OF THE PROBLEM

As shown in Figure 1, we use a fixed set of rectangular Cartesian axes with origin at the centre of the roll cover with the rubber-like layer and denote the position of a material particle in the reference configuration by X^α and the position of the same material particle in the deformed

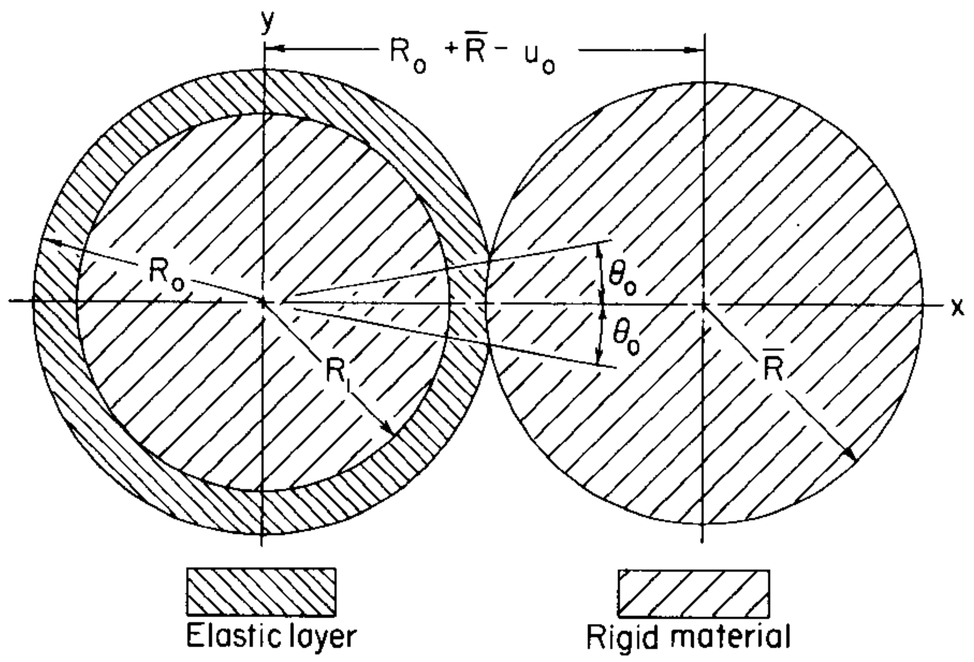

Figure 1. System to be studied

state by x_i. Thus $x_i = x_i(X^\alpha, t)$ gives the current position, at time t, of the material particle that occupied place X^α in the reference configuration. If $t = 0$ when the particle is in the reference configuration, then $x_i(X^\alpha, 0) = X^\alpha \delta_{i\alpha}$. Here $\delta_{i\alpha}$ is the Kronecker delta.

Since the core and the indentor are usually made of a material considerably harder than rubber, we regard these as being rigid and study only the mechanical deformations of the rubber-like layer. Neglecting the effect of body forces such as gravity, equations governing its deformations are

$$\rho \det F_{i\alpha} = \rho_0 \qquad F_{i\alpha} = \partial x_i / \partial X^\alpha \equiv x_{i,\alpha}$$
$$\rho \ddot{x}_i = T_{i\alpha,\alpha} \tag{1}$$

In (1), ρ is the present mass density, ρ_0 is the mass density in the reference configuration, $T_{i\alpha}$ is the first Piola–Kirchhoff stress tensor, a superimposed dot indicates material time derivative, and the usual summation convention is used. Equation $(1)_1$ is the continuity equation in the referential description. The first Piola–Kirchhoff stress tensor and the Cauchy stress tensor σ_{ij} are related by

$$\sigma_{ij} = \frac{\rho}{\rho_0} T_{i\alpha} F_{j\alpha} \tag{2}$$

Equation (1) is to be supplemented by constitutive relation for $T_{i\alpha}$ and side conditions such as boundary conditions. Before we state these, we give the assumptions made to simplify the problem.

We assume that the contact between the indentor and the roll cover is frictionless, and the effect of all dynamic forces on the deformations of the roll cover is negligible. The latter assumption is justified because the mass density of rubber is quite low, being comparable to that of water. Therefore, for practical geometries and speeds in the range of 500 r.p.m., the effect of centrifugal force on the stress distribution is very small. Following Cescotto and Fonder,[9] we assume that the rubber-like layer is made of a homogeneous material for which the strain energy density W is given by

$$W = C_1(I_1 - I_3 - 2) + C_2(I_2 - 2I_3 - 1) + \tfrac{1}{2}C_3(I_3 - 1)^2 \tag{3}$$

In equation (3), C_1, C_2 and C_3 are material constants, and I_1, I_2, I_3 are, respectively, first, second and third invariants of the right Cauchy–Green strain tensor $C_{\alpha\beta} \equiv F_{i\alpha}F_{i\beta}$ or equivalently

of the left Cauchy–Green tensor $B_{ij} \equiv F_{i\alpha}F_{j\alpha}$. We note that for incompressible materials, $I_3 = 1$ and equation (3) reduces to that for Mooney–Rivlin materials.

The constitutive assumption (3) implies that for infinitesimal deformations from the undeformed state,

$$\mu_0 = 2(C_1 + C_2) \tag{4}$$

$$\nu_0 = \frac{2C_3 - \mu_0}{4C_3 - \mu_0} \tag{5}$$

in which μ_0 is the shear modulus and ν_0 is Poisson's ratio. Thus C_3 may be regarded as a bulk modulus.

Under the aforementioned assumptions, the indentation problem becomes quasi-static and equation (1) is replaced by

$$\rho \det F_{i\alpha} = \rho_0 \tag{6}$$

$$0 = T_{i\alpha,\alpha} \tag{7}$$

$$\begin{aligned}(F^{-1})_{\alpha i}T_{i\beta} \equiv S_{\alpha\beta} &= 2(\delta_{\alpha\beta} - I_3 C^{-1}_{\alpha\beta})C_1 + 2(I_1\delta_{\alpha\beta} - C_{\alpha\beta} - 2I_3 C^{-1}_{\alpha\beta})C_2 + 2C_3 I_3 C^{-1}_{\alpha\beta}(I_3 - 1) \\ &\equiv \hat{S}_{\alpha\beta} + 2C_3 I_3 C^{-1}_{\alpha\beta}(I_3 - 1)\end{aligned} \tag{8}$$

in which $S_{\alpha\beta}$ is the second Piola–Kirchhoff stress tensor. $\hat{S}_{\alpha\beta}$ can be thought of as a deviatoric stress tensor.

In practice the length of the cylindrical rollers is significantly larger than their diameters so that it is reasonable to presume that plane strain state of deformation prevails. Thus $x_3 = \delta_{3\alpha}X^\alpha$ and equation (7) for $i = 3$ is identically satisfied. Furthermore, the deformations of the roll cover are symmetrical about the line joining the centres of the rollers. Because of this symmetry, we study the deformations of the upper half of the roll cover.

Equation (6) and the two non-trivial equations obtained by substituting (8) into (7) are three equations for three unknown fields ρ, x_1 and x_2. These equations are to be solved under the following boundary conditions. At the inner surface $X_\alpha X_\alpha = R_1$,

$$u_i = x_i - \delta_{i\alpha}X^\alpha = 0 \tag{9}$$

at the outer surface $X_\alpha X_\alpha = R_0$,

$$e_i T_{i\alpha} N_\alpha = 0 \tag{10}$$

$$\begin{aligned} n_i T_{i\alpha} N_\alpha &= 0, \qquad \text{if } \theta = \arctan\frac{X_2}{X_1} > \theta_0 \\ &= f(\theta), \quad \text{if } \arctan\frac{X_2}{X_1} < \theta_0 \end{aligned} \tag{11}$$

$$f(\theta_0) = 0$$

and at the plane thrc igh the centre line of rollers,

$$\begin{aligned} u_2 &= 0 \\ T_{12} &= 0 \end{aligned} \tag{12}$$

In equations (9)–(12), N_α is an outward unit normal to the surface in the reference configuration, e_i is a unit tangent vector to the surface in the current configuration, and n_i is a unit outward

normal to the surface in the current configuration. The boundary condition (9) implies that there is perfect bonding between the core and the rubber-like layer, and the boundary conditions (10) and (11) signify that the part of the roll cover not in contact with the indentor is traction free whereas that in contact with the indentor has a normal pressure acting on it. Note that θ_0 defines half nip width in the reference configuration. The boundary condition $(11)_3$ ensures that a contact problem rather than a punch problem is being solved.

We note that the half nip width θ_0 and the pressure $f(\theta)$ at the contact surface are unknown and are to be determined as a part of the solution. These two should assume values such that the deformed surface of the rubber-like layer matches with the profile of the indentor. In practice the load P, given by

$$P = 2\int_0^{\theta_0} f(\theta)\,\mathrm{d}\theta \tag{13}$$

pressing the two rolls together is specified. However for ease in computation, we prescribe θ_0 and find the required load. Of course one could equally well prescribe the indentation u_0, as is done in Reference 11, between the two rolls and compute the necessary load. Specification of P and then finding θ_0 and the indentation u_0, though feasible, results in significantly more computing time. The indentation u_0, shown in Figure 1, equals the distance through which the two rolls move closer when loaded and is the value of the radial displacement of that point on the outermost surface of the roll cover that lies on the centre line of the rollers.

The problem as just formulated is too difficult to solve analytically, so we solve it by the finite element method.

BRIEF DESCRIPTION OF THE FINITE-ELEMENT FORMULATION

We use the total Lagrangian formulation and the variational principle proposed by Cescotto and Fonder.[9] That is, the functional

$$H = \int \{C_3[\phi(I_3-1)-\tfrac{1}{2}\phi^2]+\hat{W}(\hat{I}_1,\hat{I}_2)\}\,\mathrm{d}V - \int h_\alpha u_\alpha\,\mathrm{d}A \tag{14}$$

where

$$\phi \equiv I_3 - 1 \tag{15}$$

$$\hat{W}(\hat{I}_1,\hat{I}_2) \equiv C_1(\hat{I}_1-3)+C_2(\hat{I}_2-3) \tag{16}$$

$$\hat{I}_1 \equiv I_1-(I_3-1) \tag{17}$$

$$\hat{I}_2 \equiv I_2-2(I_3-1) \tag{18}$$

takes an extremum value for all admissible displacements that satisfy the displacement boundary condition. In (14), h_α is the surface traction acting on a unit area in the reference configuration. Note that in taking the variation of H, both ϕ and $\mathbf{u}$ are taken as independent variables. $\delta H = 0$ gives

$$\int (I_3-1-\phi)\delta\phi\,\mathrm{d}V = 0 \tag{19}$$

$$\int (\hat{S}_{\alpha\beta}+2C_3I_3\phi C^{-1}_{\alpha\beta})\delta E_{\alpha\beta}\,\mathrm{d}V - \int h_\alpha\delta u_\alpha\,\mathrm{d}A = 0 \tag{20}$$

in which

$$E_{\alpha\beta} = (C_{\alpha\beta} - \delta_{\alpha\beta})/2$$

We assume that the load $f(\theta)$ at the contact surface is applied in M equal increments and denote the incremental change in the value of say $\mathbf{u}$ caused by the $(N+1)$st load step by $\Delta\mathbf{u}$, i.e.

$$\mathbf{u}^{N+1} = \mathbf{u}^N + \Delta\mathbf{u}, \qquad \mathbf{E}^{N+1} = \mathbf{E}^N + \Delta\mathbf{E}, \qquad \phi^{N+1} = \phi^N + \Delta\phi. \tag{21}$$

From equations $(9)_1$, (21), and the expression for $\mathbf{C}$ in terms of $\mathbf{F}$, we obtain

$$\begin{aligned} \Delta E_{\alpha\beta} &= \Delta e_{\alpha\beta} + \Delta\eta_{\alpha\beta} \qquad \Delta\eta_{\alpha\beta} = \tfrac{1}{2}\Delta u_{\gamma,\alpha}\Delta u_{\gamma,\beta} \\ \Delta e_{\alpha\beta} &= \tfrac{1}{2}(\Delta u_{\alpha,\beta} + \Delta u_{\beta,\alpha} + u^N_{\gamma,\alpha}\Delta u_{\gamma,\beta} + u^N_{\gamma,\beta}\Delta u_{\gamma,\alpha}) \end{aligned} \tag{22}$$

Recalling that $\Delta I_3 = 2(C^N)^{-1}_{\alpha\beta}\Delta E_{\alpha\beta}$, we obtain from (8),

$$\Delta\hat{S}_{\alpha\beta} = -4(C_1 + 2C_2)[(C^N)^{-1}_{\gamma\delta}(C^N)^{-1}_{\alpha\beta}\Delta E_{\gamma\delta} - 2I_3{}^N(C^N)^{-1}_{\alpha\gamma}(C^N)^{-1}_{\beta\delta}\Delta E_{\gamma\delta}] + 8C_2[\Delta E_{\gamma\gamma}\delta_{\alpha\beta} - \Delta E_{\alpha\beta}] \tag{23}$$

Setting $\delta E_{\alpha\beta} = \delta\Delta E_{\alpha\beta}$, $\delta u_\alpha = \delta\Delta u_\alpha$ and $\delta\phi = \delta\Delta\phi$ in (19) and (20) we obtain

$$\int \{I_3^N + 2I_3^N(C^N)^{-1}_{\alpha\beta}\Delta E_{\alpha\beta} - 1 - \phi^N - \Delta\phi\}\delta\Delta\phi \, \mathrm{d}V = 0 \tag{24}$$

$$\begin{aligned} &\int [(\hat{S}^N_{\alpha\beta} + \Delta\hat{S}_{\alpha\beta}) + 2C_3(\phi^N + \Delta\phi)(I_3^N + \Delta I_3)(C^N)^{-1}_{\alpha\beta} \\ &\quad - 2(C^N)^{-1}_{\alpha\gamma}(C^N)^{-1}_{\beta\delta}\Delta E_{\gamma\delta}]\delta\Delta E_{\alpha\beta} \, \mathrm{d}V - \int h^{N+1}_\alpha \delta\Delta u_\alpha \, \mathrm{d}A = 0 \end{aligned} \tag{25}$$

We now make the assumption that the increment in the load is small so that

$$\Delta\hat{S}_{\alpha\beta}\delta\Delta E_{\alpha\beta} \simeq \Delta\hat{\hat{S}}_{\alpha\beta}\delta\Delta e_{\alpha\beta} \tag{26}$$

$$(C^N)^{-1}_{\alpha\beta}\Delta E_{\alpha\beta} \simeq (C^N)^{-1}_{\alpha\beta}\Delta e_{\alpha\beta} \quad \text{etc} \tag{27}$$

$\Delta\hat{\hat{S}}_{\alpha\beta}$ is obtained from $\Delta\hat{S}_{\alpha\beta}$ by replacing $\Delta E_{\alpha\beta}$ in (23) by $\Delta e_{\alpha\beta}$. Equations (24) and (25) are approximated by the following:

$$\int I_3^N (C^N)^{-1}_{\alpha\beta}\Delta e_{\alpha\beta}\delta\Delta\phi \, \mathrm{d}V \simeq -\tfrac{1}{2}\int (I_3^N - 1 - \phi^N)\delta\Delta\phi \, \mathrm{d}V \tag{28}$$

$$\begin{aligned} &\int \Delta\hat{\hat{S}}_{\alpha\beta}\delta\Delta e_{\alpha\beta} \, \mathrm{d}V + \int S^N_{\alpha\beta}\delta\Delta\eta_{\alpha\beta} \, \mathrm{d}V + 2C_3\int I_3^N(C^N)^{-1}_{\alpha\beta}\Delta\phi\delta\Delta e_{\alpha\beta} \, \mathrm{d}V \\ &\quad \simeq \int h^{N+1}_\alpha \delta\Delta u_\alpha \, \mathrm{d}A - \int S^N_{\alpha\beta}\delta\Delta e_{\alpha\beta} \, \mathrm{d}V \end{aligned} \tag{29}$$

Equilibrium iterations,[12] i.e. iterations within a load step, are used to ensure that equilibrium equations (28) and (29) are satisfied within a prescribed error.

A finite element computer program based on equations (28) and (29) and employing 4-node isoparametric quadrilateral elements with 2×2 Gaussian integration rule has been written. The dilatation ϕ is assumed to be constant within each element. The pressure load between two surface nodal points a and b is replaced by lumped nodal loads given by

$$h^a_i = h^b_i = f(\theta^*)\varepsilon_{3ij}(x^b_j - x^a_j)/2 \tag{30}$$

Here ε_{ijk} is the permutation symbol and it equals 1 or -1 according as i, j, k form an even or an odd permutation of 1, 2 and 3 and is zero otherwise, and θ^* is the value of θ for the midpoint of the line joining nodes a and b. The loads for the $(N+1)$th load step are calculated based upon the positions of the nodes after the Nth load step.

The accuracy of the developed finite element code has been established by comparing computed results with those obtained from the analytical solution for the pressure vessel problem. When the material of the pressure vessel is incompressible, the finite strain problem was studied, whereas the infiinitesimal strain problem was analysed when the pressure vessel is made of a compressible material.

COMPUTATION AND DISCUSSION OF RESULTS

In order to solve the title problem by the finite element method, we consider the quarter of the roll cover in the first quadrant and explore the effect of boundary conditions on the vertical plane. The two sets of results obtained first with the vertical plane taken as traction free and then constrained not to move horizontally were virtually indistinguishable. This is so because both the stresses and displacements decay rather rapidly with the distance from the contact region. This was found to be true in the previous studies[1–3] and is confirmed by the results obtained herein. The quarter of the roll cover is divided into quadrilateral elements as shown in Figure 2. The mesh is finer within approximately one and a half times the contact width.

Half nip width θ_0 and the form of the function $f(\theta)$ are assumed. The presumed load is divided into 20 equal steps and within each load step up to 15 equilibrium iterations are performed to ensure that displacements are accurate to within 1 per cent of their values. The deformed surface of the roll cover is calculated and a check is made to ensure that the deformed surface in the assumed contact zone matches, within a specified tolerance, with the circular profile of the indentor and that the nodal point just outside the presumed contact area has not penetrated into the indentor. If the second condition is not satisfied implying thereby that

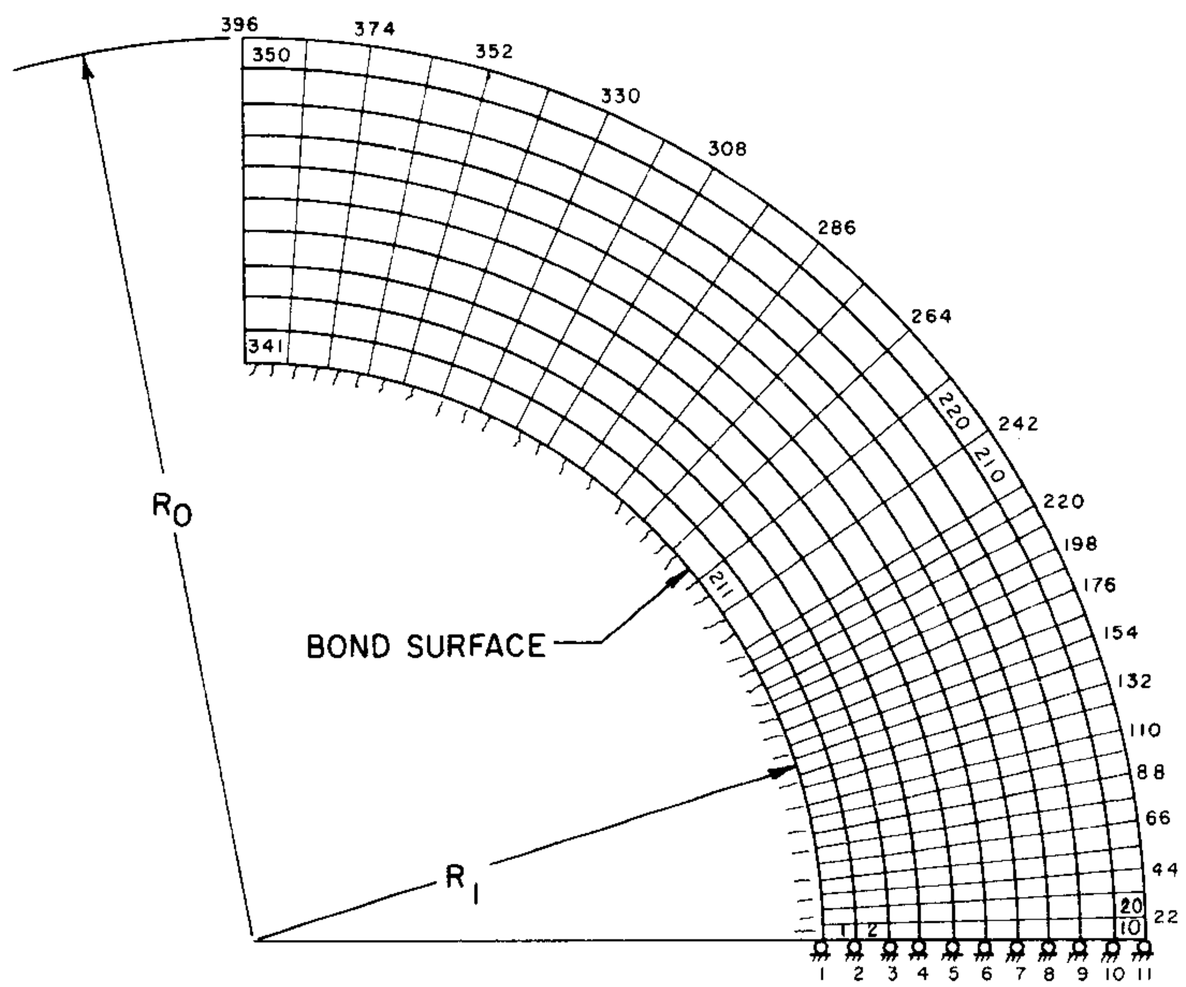

Figure 2. Finite element grid

the assumed contact width is too small, either the value of θ_0 is increased or the total load is decreased. However, if the second condition is satisfied but the first is not, the form of $f(\theta)$ is suitably modified until both preceding conditions are simultaneously met. The deformed surface of the roll cover is taken to match with the profile of the indentor if the distance of each nodal point on the contact surface from the indentor is within 1 per cent of the indentation u_0. Usually, with a little experience, one can make pretty good estimates of θ_0 and $f(\theta)$ so that the entire process converges in four or five iterations.

In the results presented and discussed below, the value of θ_0, the semi-contact width in the reference configuration, is kept constant. For results obtained by using a linear theory, the entire load is applied in one step on the undeformed surface. Also the strain–displacement relation and the stress–strain relations are linear. In the nonlinear theory, the problem is solved incrementally and each increment in load is applied on the surface deformed up to the application of that load increment. Results for the compressible case are computed by setting Poisson's ratio, ν_0, in the undeformed state equal to 0·45. Both for compressible and incompressible cases, $C_1 = 13{\cdot}79\ \text{N/cm}^2$, $C_2 = 3{\cdot}45\ \text{N/cm}^2$, and the value of C_3 is determined from equation (5). To model the rubber as an incompressible material, C_3 is set equal to $4320\ \text{N/cm}^2$. The values of various geometric parameters correspond to those for run number 30 of Spengos.[4] That is $R_1 = 47{\cdot}2$ mm, $R_0 = 60{\cdot}7$ mm, $\bar{R} = 76{\cdot}2$ mm. The results presented for the incompressible case in which the rubber-like layer is modelled as a Mooney–Rivlin material are taken from Reference 3.

Figure 3 depicts the pressure profile at the contact surface for various cases. As expected, considerably less load is required to indent the compressible layer than an incompressible one. For the particular situation under consideration, the load required for the compressible case is 77 per cent of that required when the rubber-like covering layer is assumed to be

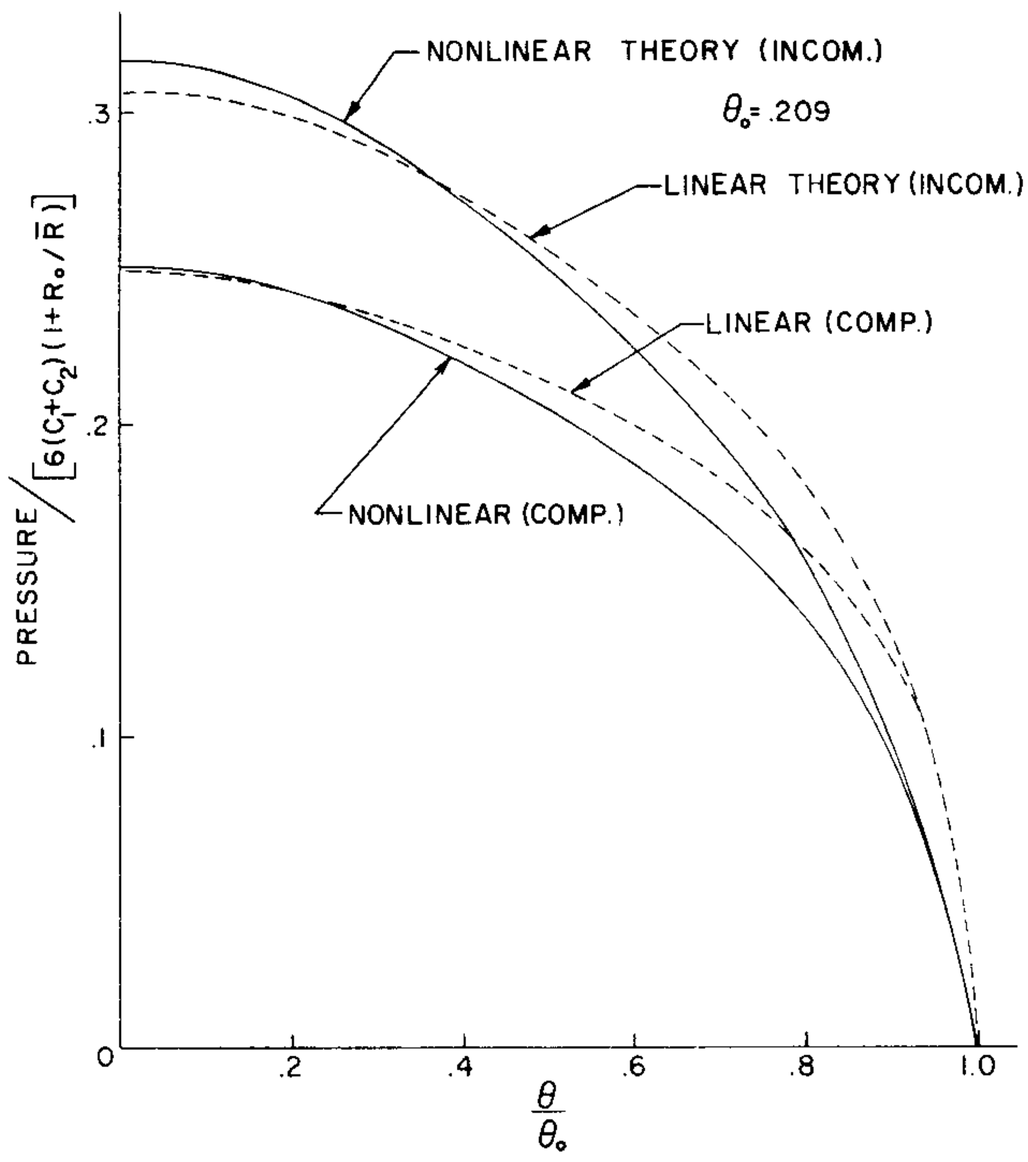

Figure 3. Stress distribution at the contact surface

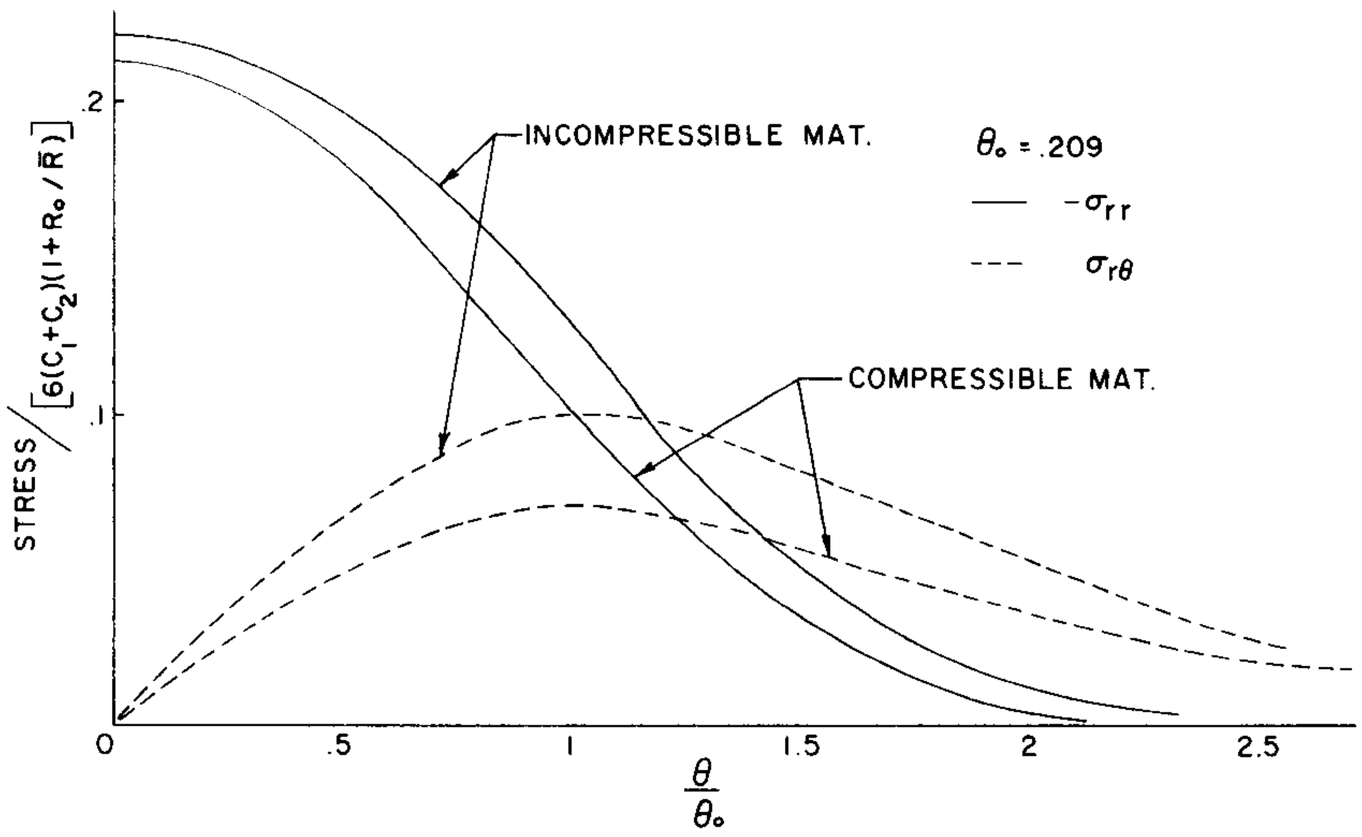

Figure 4. Stress distribution at the bond surface

incompressible. The contact width in the deformed shape for the compressible layer is 92 per cent of that for the incompressible layer. We remark that the pressure profile at the contact surface represents the non-dimensionalized Cauchy stress.

Results presented in Figure 4 verify the assumption that stresses decay rapidly at points away from the contact zone. The magnitudes of developed shear stresses at the bond surface seem to indicate that the glued joint will hold better when the rubber-like layer is made of a compressible material.

In Figure 5 is shown half of the deformed surface of the roll cover; also, due to different scales along the horizontal and vertical axes, the undeformed and deformed roll cover as well

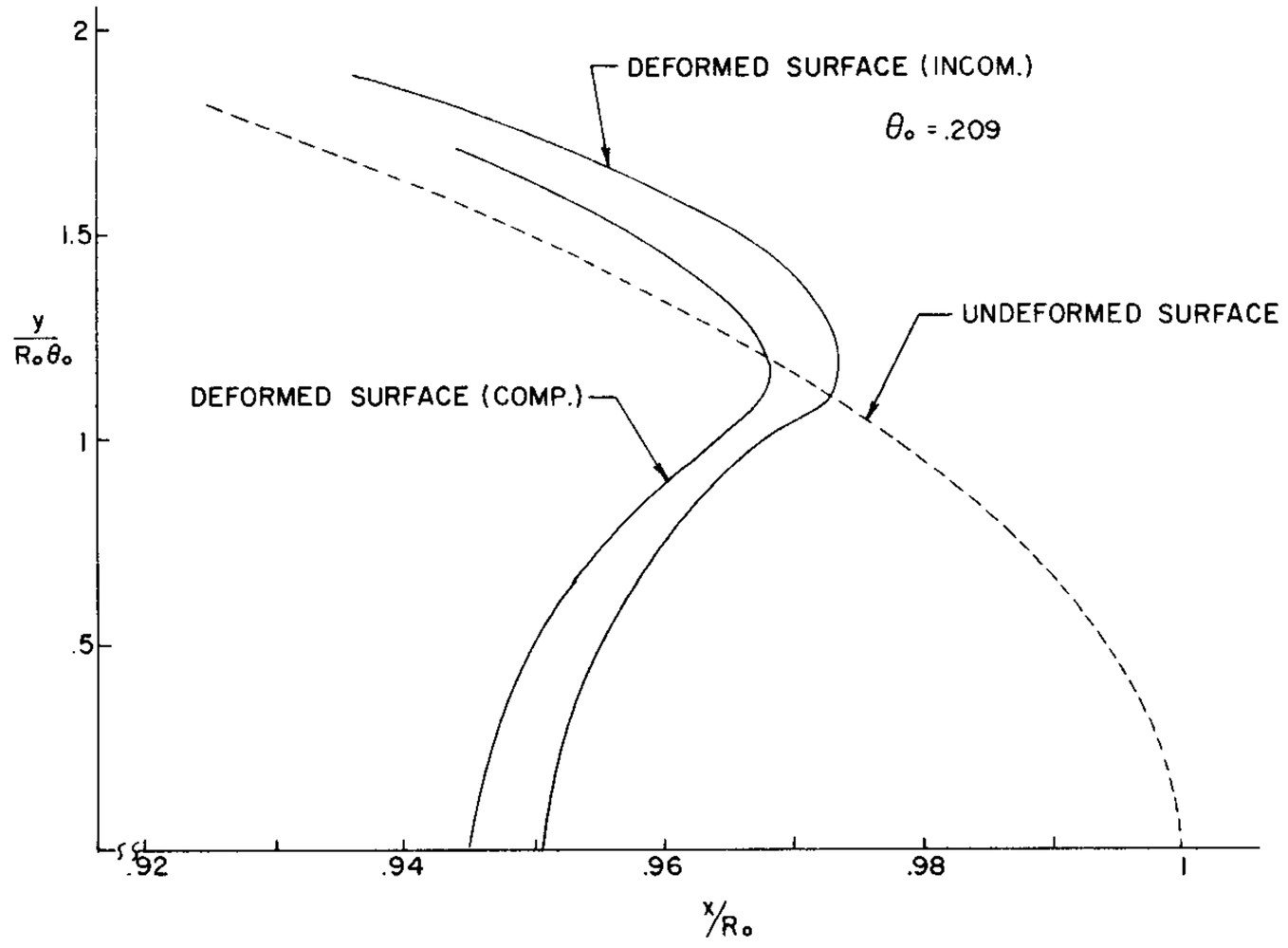

Figure 5. Deformed surface of the rubber-like layer

as the indentor plot as ellipses. The radius of curvature of the deformed surface near the point where rubber leaves the indentor is different in the two cases. In certain applications, for example, paper industry, this can play a major role in the design of roll covers. Finally, in Figure 6 the computed non-dimensionalized pressure profile on the contact surface is compared with that obtained experimentally by Spengos. Computed results are those obtained by using the nonlinear theory. From the results presented in Figure 6, it seems that the rubber used by Spengos in his experimental set up was incompressible. The difference between the calculated results and experimental ones is possibly due to the fact that the assumption of plane strain state of deformation made in the analysis is not quite valid for Spengos' experimental set up wherein the length to diameter ratio of rollers was of the order of one. In Figure 6, a denotes the semicontact width in the current configuration.

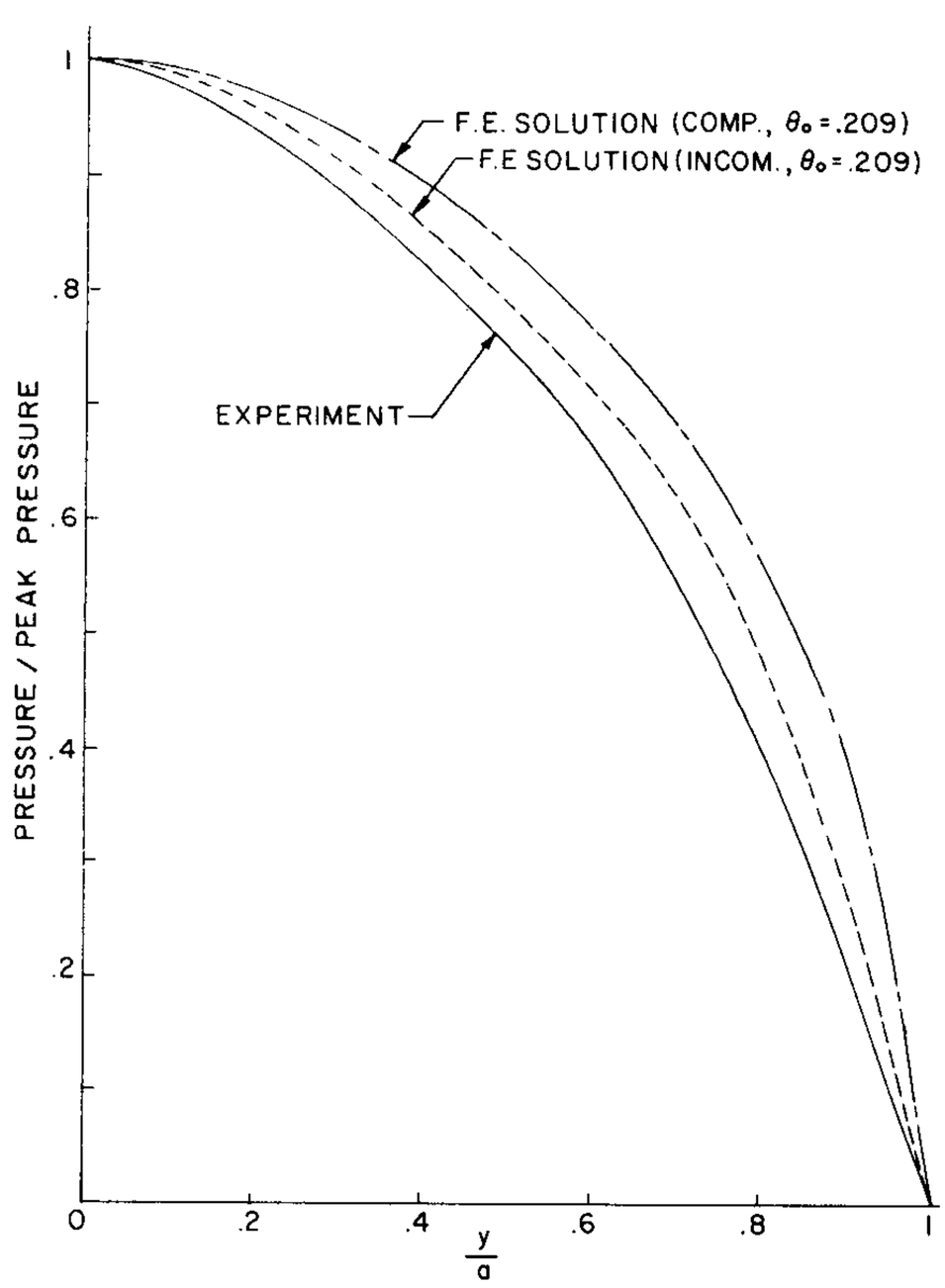

Figure 6. Stress distribution at the contact surface: comparison of experimental and numerical results

REMARKS

Upon writing equation (8) explicitly for the plane strain case, we see that the values of S_{11}, S_{22} and S_{12} and hence of σ_{11}, σ_{22} and σ_{12} depend upon the material constants C_1 and C_2 only through their sum. Since for plane strain case S_{33} does not contribute to the strain-energy density, hence the values of displacements also depend upon C_1 and C_2 only through C_1+C_2. Thus results presented herein are valid for all values of C_1/C_2 so long as the sum C_1+C_2 is kept constant. The value of the stress σ_{33} normal to the plane of deformation does depend upon C_1/C_2 even when C_1+C_2 is kept fixed.

We solve the contact problem by first presuming the contact width and estimating a pressure profile on it and then verifying that the assumed contact width is indeed correct. Hung and de Saxce[13] incorporate the condition that the normal pressure on the contact surface be positive into the variational principle and reduce the elastic contact problem to a special case of the mathematical programming technique. Their analysis applies to infinitesimal deformations of a linear elastic body in contact with another linear elastic body.

A finite element computer program based on equations (28) and (29) and employing 8-node isoparametric elements was also written. The dilatation was assumed to be constant within each element. Both 3×3 and 2×2 Gaussian integration rules were used. For the thick-wall pressure vessel problem this computer code gave accurate values of the displacement but the stresses oscillated considerably from one Gauss point to another Gauss point within an element and from one element to the adjoining element. It seems that the assumption that the dilatation is constant within an element is not valid for the 8-node isoparametric element. The case when the dilatation is assumed to vary linearly within the 8-node isoparametric element has not been incorporated into the computer code yet.

CONCLUSIONS

Results presented in Figure 3 reveal that, for the problem studied herein, the compressibility of rubber has more effect on the pressure at the contact surface than the material and geometric nonlinearities. The maximum principal strain for the nonlinear problem was 40 per cent and 22·75 per cent according as the rubber was modelled as an incompressible material or a compressible material with $\nu_0 = 0{\cdot}45$. Note that the contact width in the reference configuration is kept fixed in the two cases. Also for the same value of the contact width in the reference configuration, the indentation is 10 per cent more and the load required is 23 per cent less for the compressible rubber-like layer with $\nu_0 = 0{\cdot}45$ as compared to that for the incompressible layer.

REFERENCES

1. R. C. Batra, M. Levinson and E. Betz, 'Rubber covered rolls—the thermoviscoelastic problem. A finite element solution', *Int. J. num. Meth. Engng*, **10**, 767–785 (1976).
2. H. T. Hahn and M. Levinson, 'Indentation of an elastic layer(s) bonded to a rigid cylinder—I. Quasistatic case without friction', *Int. J. Mech. Sci.*, **16**, 489–502 (1974).
3. R. C. Batra, 'Rubber covered rolls—the nonlinear elastic problem', *J. Appl. Mech.*, **47**, 82–86 (1980).
4. A. C. Spengos, 'Experimental investigation of rolling contact', *J. Appl. Mech.*, **32**, 859–864 (1965).
5. P. Meijers, 'The contact problem of a rigid cylinder on an elastic layer', *Appl. Sci. Res.*, **18**, 353–383 (1968).
6. Dennis P. Skala, 'Large strain finite element analysis for a compressible elastomeric material', *Proc. Symp. Appl. Comp. Meth. Engng*, Los Angeles, 1977, 1095–1103.
7. D. J. Naylor, 'Stresses in nearly incompressible materials by finite elements with applications to the calculation of excess pore pressures', *Int. J. num. Meth. Engng*, **8**, 443–460 (1974).
8. T. J. Hughes, R. L. Taylor and J. L. Sackman, 'Finite element formulation and solution of contact and impact problems in continuum mechanics—III', *Report 75–7*, Univ. of California, Berkeley (1975).
9. S. Cescotto and G. Fonder, 'A finite element approach for large strains of nearly incompressible rubberlike materials', *Int. J. Solids Struct.* **15**, 589–605 (1979).
10. A. E. Green and W. Zerna, *Theoretical Elasticity*, 2nd edn, Oxford Univ. Press, London, 1968.
11. R. C. Batra, 'Cold sheet rolling; the thermoviscoelastic problem, a numerical solution', *Int. J. num. Meth. Engng*, **11**, 671–682 (1977).
12. L. D. Hofmeister, G. A. Greenbaum and D. A. Evensen, 'Large strain elasto-plastic finite element analysis', *AIAA J.*, **9**, 1248–1254 (1971).
13. Nguyen Dang Hung and Gery de Saxce, 'Frictionless contact of elastic bodies by finite element method and mathematical programming technique', *Computers Struct.*, **11**, 55–67 (1980).